Standalone Real-Time Positioning Algorithm Based on Dynamic Ambiguities (DARTS)

Andrew Simsky, *Septentrio*

BIOGRAPHY

Dr Andrew Simsky holds a Ph.D. in physics from the University of Moscow (Russia). He is working as a senior GNSS scientist at Septentrio in Leuven, Belgium. His research interests include differential and standalone navigation algorithms and performance analysis of GNSS receivers. He previously worked on carrier-phase DGPS algorithms for airborne gravimetry at Sander Geophysics Ltd in Ottawa, Canada.

ABSTRACT

This paper presents an original navigation algorithm intended to push the accuracy of standalone positioning beyond the limitations imposed by GPS system biases (errors of broadcast orbits and clocks). The proposed algorithm is based on the processing of iono-free carrier-phase combination with floating ambiguities by the Kalman filter. Unlike traditional phase processing, ambiguities are essentially modeled as dynamic values intended to absorb long-term range errors, of which GPS system biases are the most essential. The model, which describes the behavior of ambiguities, has been optimized using both experimental and simulated data sets. The acronym DARTS reads as **D**ynamic **A**mbiguities **R**eal-**T**ime **S**tandalone.

The accuracy of DARTS is close to typical accuracies of code-based DGPS. Standard deviations for position are within the range of 1.0-1.3m for heights, and 0.6-0.8 m for horizontal coordinates. This level of accuracy has been proven for a variety of applications.

DARTS has been designed having in mind its application in GNSS receivers. Its implementation for the new firmware version of Septentrio's GNSS receiver, PolaRx2, is currently underway.

INTRODUCTION

After SA has been turned off in May 2000, single-point positioning algorithms using iono-free carrier phase processing with floating ambiguities have gotten significant attention. In [1] it has been shown that decimeter-level accuracy can be achieved when post-mission precise orbits and 30-sec clock corrections are used. However, such algorithms can be used only for post-processing, when precise IGS products become available.

For real-time single-point applications, navigation algorithms are subjected to GPS system biases, i.e., errors of broadcast orbits and clocks, also called user range errors (URE). System biases are traditionally considered as an inevitable contribution to the error budget of single-point positioning and result in positional errors of 2-5 meters. The only way to improve the positional accuracy of non-assisted real time single-point positioning is to estimate GPS system biases in real-time and apply these corrections to GPS observations. This is exactly what DARTS is designed for. In order to estimate system biases and compensate for them in real-time, DARTS employs the concept of dynamic ambiguities.

According to the traditional formulation of carrier phase processing, floating ambiguities are modeled as constant values and hence are expected to show converging behavior. In DARTS, ambiguities are modeled as non-constant, slowly changing values, and their expected behavior is to follow the long-term variations of range errors. The way of estimating system biases is, therefore, implicit: the variations of biases are absorbed by variations of dynamic ambiguities.

The effectiveness of DARTS can be best appreciated by comparing it to DGPS. Indeed, in differential processing system biases are fully canceled (except for a small residual effect of orbit errors). With DARTS, only partial compensation of system biases can be achieved. It is shown further in this article that the accuracy of DARTS is comparable to the accuracy of DGPS, and therefore it can be concluded that a substantial portion of system biases is compensated by DARTS.

In the following sections the principle of DARTS is described in detail. Optimization of DARTS is illustrated

by using actual and simulated data sets. The performance of DARTS is verified for a variety of applications.

PRINCIPLE OF DARTS

DARTS in its current implementation is based on joined processing of iono-free code and phase pseudoranges by the Kalman filter. This section contains the brief description of measurement and system noise models used by DARTS. Most of the mathematical formulation of DARTS follows the standard pattern typical for other kinds of phase processing. However, the system noise model for phase ambiguities is different from the one normally used for carrier phase processing.

Measurement noise model

The measurement vector and measurement noise matrix have a standard appearance:

$$\begin{bmatrix} \vec{\rho} \\ \vec{\varphi} \end{bmatrix} \qquad (1)$$

$$\begin{bmatrix} \sigma_\rho^2 \hat{I} & 0 \\ 0 & \sigma_\varphi^2 \hat{I} \end{bmatrix} \qquad (2)$$

Here, $\vec{\rho}$, $\vec{\varphi}$ denote the set of pseudoranges and phases for all the satellites in the solution. If the receiver clock bias is to be computed, $\vec{\rho}$, $\vec{\varphi}$ must be raw measurements; if only positional solution is sought, receiver clock bias may be excluded by choosing a base satellite and replacing simple measurements with differences:

$$\begin{bmatrix} \vec{\rho} - \rho_{base} \\ \vec{\varphi} - \varphi_{base} \end{bmatrix} \qquad (3)$$

If differenced observations (3) are used, the matrix (2) must be appropriately recomputed to take into account correlation between differenced measurements.

In DARTS, the measurement noises variances of pseudoranges and phases are set to nominal values, typical to normal phase processing, so that $\sigma_\rho^2 >> \sigma_\varphi^2$, typically $\sigma_\rho / \sigma_\varphi \cong 100$. Exact values of assumed measurement variances make little difference for the positional solution.

System noise model

DARTS is based on the standard formulation of the Kalman filter [2,3]. The full state vector $\vec{X}$ includes position $\vec{x}$, velocity $\vec{v}$ and phase ambiguities $\vec{N}$:

$$\vec{X} = \begin{bmatrix} \vec{x} \\ \vec{v} \\ \vec{N} \end{bmatrix} \qquad (4)$$

If the state vector does not include receiver clock components (which is the case in the above formula), differenced observations (3) must be used. The state vector for the current epoch is related to the state vector for the previous epoch with a standard prediction formula:

$$\vec{X}_{k+1} = \hat{A}\vec{X}_k + w \qquad (5)$$

Here w is system noise, characterized by the system noise matrix:

$$\hat{W} = \Delta t \begin{bmatrix} q_x \hat{W}_x & 0 \\ 0 & q_N \hat{I} \end{bmatrix} \qquad (6)$$

Here $\hat{W}_x$ is a usual kinematic 6x6 system noise matrix [3]; q_x is a parameter, which characterizes the dynamics of the system. The role of q_x is well known: low values of q_x indicate slowly moving system with low dynamics, while high values of q_x indicate the system with highly dynamic movement. For static positioning, q_x is usually set to a very low value, limited only by considerations of numeric stability. For each dynamic system there exists an optimal value of q_x, which characterizes the best achievable compromise between the suppression of measurement noise and representation of actual movement.

The value of q_N, which plays the central role in DARTS, characterizes the behavior of ambiguities in exactly the same way in which q_x characterizes the kinematic behavior of the system. In other words, q_N characterizes the value of system noise in an update formula for ambiguities:

$$\vec{N}_{k+1} = \vec{N}_k + w_N \qquad (7)$$

In the traditional formulation of carrier phase processing, q_N is set to a very small value, which corresponds to the assumption that formula (7) is precise ($w_N = 0$) and ambiguities are real constants. The resulting behavior of ambiguities is quite analogous to the behavior of the positional solution in the case of static positioning: ambiguities are converging to constants and their variance decreases with time.

Applying the model of constant ambiguities to single point positioning affected by GPS system biases would be as inadequate as attempting to describe low-frequency oscillation with a static positioning model. As for each dynamic system there exists an optimal setting of the q_x, which characterizes dynamic behavior of the system, there also exists an optimal setting of q_N, which fits best actual behavior of GPS system biases. This optimal value characterizes GPS as a system and does not depend upon time, location or a kind of application. Optimization of q_N, the spectral density of system noise for ambiguities, is a subject of the following sections.

OPTIMIZATION OF DARTS

Optimization of DARTS is done with actually collected GPS data sets. However, we found that simulated sets of GPS observations can be very useful to better understand the nature of DARTS, its internal working, and its performance in different situations. We begin this section with the description of our simulation methodology.

Simulation of system biases

Software simulation of system biases provides a useful tool to look into the mechanism of DARTS and investigate the behavior of the algorithm in various conditions. One definite advantage of the software simulation is a possibility to deal with system biases alone, purified from multipath, tracking, and atmospheric errors.

For the purposes of this paper 24-hour static data sets have been simulated with a data rate of 1 sec. Tracking noise, multipath and all the physical biases, such as propagation delays, relativistic effects, Earth rotation, etc, were neglected. Both pseudoranges and phases were simulated with the help of the same formula:

$$\vec{\rho}, \vec{\varphi} = computed\ ranges + A\sin\left(\frac{2\pi t}{T} + \delta_{prn}\right) \quad (8)$$

The purpose of this simple model is to capture the most essential behavior of DARTS solutions. According to this model, pseudoranges and phases are equal. The differences between code and phase are introduced at the stage of processing in two ways: by using different noise variances according to the noise model (2) and by using ambiguities for phase.

According to model (8), the amplitude of the biases is the same for all the satellites, but the phase is shifted in a quasi-random way, so that the biases for different PRNs oscillate with a different phase shift (see, as an example, Figure 2). The computed ranges were calculated using an actual daily navigation file from IFAG, day 183 of year 2003 and the actual location of Septentrio in Leuven, Belgium. The period of biases, T, took values of 6, 12, and 24 hours. The case of constant biases, which corresponds to $T = \infty$, was also considered. In this case the values of biases were randomized.

Below we shall look at the behavior of positional solutions obtained by DARTS for both real and simulated data sets.

Optimization of q_N

Optimization of q_N, the spectral density of system noise for ambiguities, is a central concept of DARTS. Positional accuracy of DARTS depends upon the value of q_N. When q_N scans the range of available values, the optimal value of q_N is the one, which furnishes the lowest possible RMS of positional solution. This optimal value characterizes the dynamics of system biases and does not depend upon time, location, or a kind or application.

When the value of q_N is increased, ambiguities are made more flexible. The limit of very high values ($q_N = \infty$) corresponds to the case of code-only processing, when ambiguities are updated afresh every epoch. When the value of q_N is reduced, ambiguities are made more "rigid". The limit of very low values ($q_N = 0$) corresponds to the case of usual phase processing with constant (converging) ambiguities.

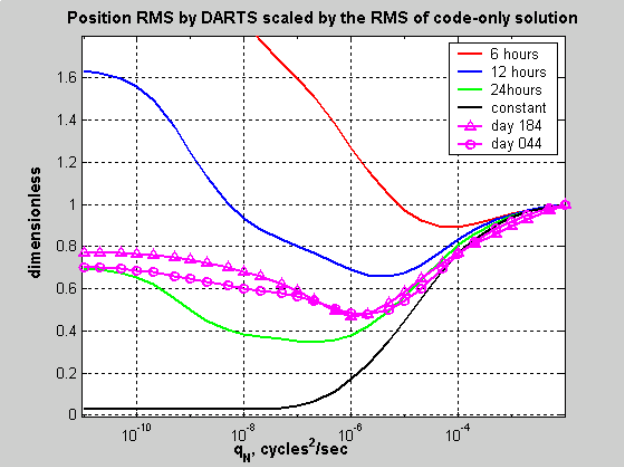

Figure 1. Optimization of q_N for simulated and real data sets. Curves without symbols correspond to simulated data sets with different T. Magenta curves with symbols correspond to real data sets. Optimal q_N correspond to the minima of the curves.

Figure 1 illustrates the optimization of q_N for both simulated and real data sets. Plotted in the figure is the ratio of the total RMS of position computed by DARTS to the total RMS of the code-only solution (limit $q_N = \infty$). Therefore all the curves coincide at the right edge of the plot. This scaling provides a natural way to plot together optimization curves for simulated and real data sets. For simulated scenarios, the amplitude of biases (*A* in formula (8)) is an arbitrary value; therefore the values of positional errors must be reduced to a dimensionless form in order to be comparable to positional errors for real data sets.

Due to the chosen method of scaling, Figure 1 directly shows the effect of DARTS. Indeed, the plotted values indicate the gains in accuracy achieved by using phase instead of using only code. Most of the curves have clear minima, which correspond to the optimal values of q_N.

The only curve without a minimum (the black one) corresponds to the simulated data set with constant biases. The black curve shows, in accordance with expectations, that with constant biases the model of constant ambiguities is the most adequate. It is worth notice that in this case the accuracy comes to cm-level values typical for differential phase processing. This means that absorption of constant biases by constant ambiguities is indeed quite efficient: the errors of code processing are reduced more that by an order of magnitude.

All the other simulated curves have clear minima. The shorter the period of biases, the greater is the value of q_N, which furnishes the minimal positional error. This is logical because reducing of T is equivalent to increasing the dynamics of the system. With higher dynamics of the system biases, higher values of the system noise variance are required for optimal performance.

The values of the minima indicate the effectiveness of phase aiding. It can be seen that the depth of the minima increases with the period T. This means, in accordance with expectations, that the higher the dynamics, the less effective is phase aiding: phase ambiguities do not have enough time to adjust to quickly changing biases. For the highest-frequency scenario (T = 6 hours), the positional RMS error of the best DARTS solution is only by 10% less than the positional RMS error for the code-only solution. For the slowest scenario (T = 24 hours) the phase aiding is the most effective: the positional RMS error of the optimal DARTS solution is almost 3 times as low as for the code-only solution.

Please note that our simulated solutions are not affected by error sources specific for real code pseudoranges, such as code multipath or tracking errors. Therefore our simulation provides a way to observe the effects of dynamic ambiguities in a pure form, to separate these effects from a more trivial mechanism of code smoothing with phase.

Figure 1 shows that the simulated optimization curve for the period T=24 hours is the closest to the optimization curves for real data sets. This curve also has one important feature in common with the optimization curves for real data: the positional RMS at the limit of $q_N \to 0$ (limit of constant ambiguities) is lower than the positional RMS at the limit of $q_N \to \infty$ (code-only processing). This means that for both real data and the simulation at T = 24 hours, phase processing with constant ambiguities is more accurate than code-only processing. Due to this apparent similarity we consider the simulation scenario with a period of T = 24 hours as a close analog of the real data sets.

Figure 1 also shows that the optimization curves for actual data sets are close to each other and indicate apparent existence of an optimal value of q_N. The optimal value chosen for the final implementation is 5.0E-6. Due to the flatness of all the optimization curves in the vicinity of the minima, it is obvious that the final results of DARTS are relatively insensitive to the particular value of q_N as long as this value is somewhere between 1.0E-6 and 1.0E-5. Despite individual differences between data

sets due to time, location, etc., the same value of optimal q_N furnishes a close to optimal performance for all of them.

Absorption of range errors by DARTS ambiguities

Of all the four simulated data sets, the one with the period of biases of 24 hours provides the results the most similar to the actual data sets. In this subsection this data set is used to illustrate the absorption of system biases by phase ambiguities.

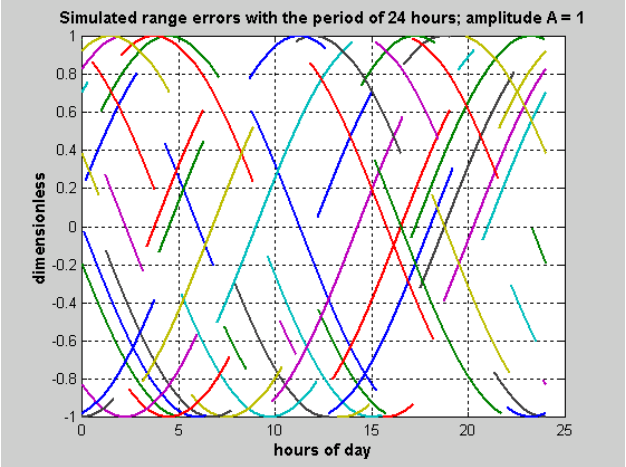

Figure 2. Simulated biases by formula (8) with the period T = 24 hours. According to our results, these biases capture essential traits of real orbit and clock errors of GPS satellites.

Figure 2 shows the simulated biases computed by formula (8) for the period of 24 hours. According to our results, these biases capture most essential traits of the behavior of real GPS system biases.

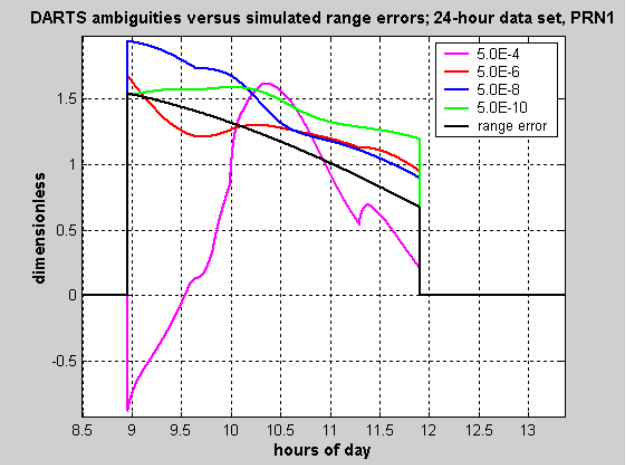

Figure 3. Absorption of simulated range biases by DARTS ambiguities for different values of q_N; PRN1.

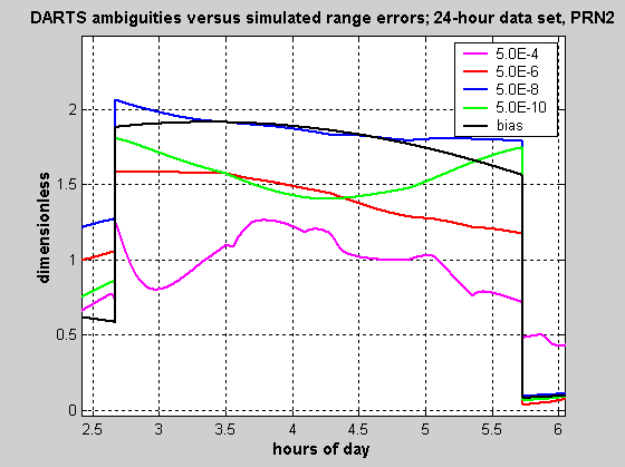

Figure 4. Absorption of simulated range biases by DARTS ambiguities for different values of q_N; PRN2.

Figure 3-Figure 5 show how well the DARTS ambiguities follow simulated system biases. In this plots the black curves show code residuals of static processing with fixed position; these residuals contain only simulated range errors. Colored curves show DARTS ambiguities at different values of q_N. Both static residuals and ambiguities were computed in the processing with a base satellite (an analog of "double-differencing" for single-point positioning). These values may exceed the amplitude of simulated biases (the value of 1), and jumps may occur at the moments when base satellites are switched. Please notice that the values in Figure 3-Figure 5 are scaled by the value of *A*, the amplitude of the oscillating biases.

Figure 3-Figure 5 as well as similar plots for the other satellites show that DARTS ambiguities follow the variations of range errors with decimeter-level precision (the scale of the Y-axis of the plots roughly corresponds to meters). According to Figure 1, the range of optimal q_N for the T = 24 hour is between 1E-6 and 1E-8. That is why the performance of ambiguities is the best for the value of q_N = 5E-8, which belongs to this range.

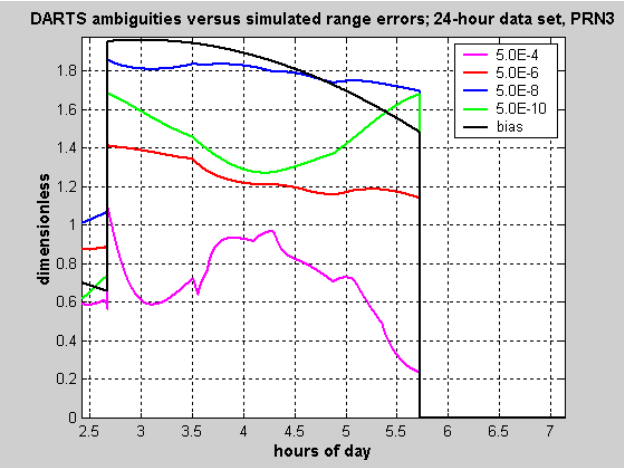

Figure 5. Absorption of simulated range biases by DARTS ambiguities for different values of q_N ; PRN3.

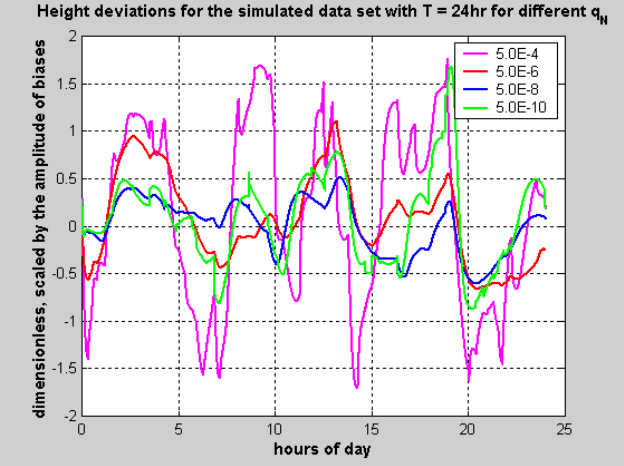

Figure 6. Height deviations by DARTS at different values of q_N for the simulated data set with the period T = 24 hours.

Figure 6 shows actual performance of DARTS positional solution for different values of q_N . Again, as expected, the value of q_N = 5E-8 furnishes the best performance. The magenta curve in Figure 6 corresponds to the code-only solution. The blue curve corresponds to the optimal DARTS. When these two curves are compared, it can be seen that the DARTS solution follows the same trends as the code-only solution, but the amplitude of the deviations is substantially reduced (in this case by a factor of 3 on average). Further in this paper we shall observe similar behavior for real data sets.

VERIFICATION OF DARTS

In this section we present the performance of DARTS for a few sample applications. Table 1contains a summary of positional performance for four test cases. It can be seen that DARTS shows stable performance with sub-meter horizontal errors and around-one-meter height errors for different locations and a variety of applications.

	Static tests		Kinematic tests	
	Leuven, Belgium	Ottawa, Canada	Aircraft	Container terminal
Height	1.3	1.33	0.92	0.69
North	0.72	0.81	0.47	0.38
East	0.84	1.06	0.55	0.45
Horizontal	1.12	1.34	0.72	0.59
Total 3D	1.71	1.88	1.17	0.91

Table 1. RMS deviations of positional solution by DARTS for a few test cases, meters.

Velocities computed by DARTS have mm/sec-level noise typical for RTK. The noise of velocities computed by DARTS is about the same as for the velocities directly computed from Doppler measurements (see [4] for more details on velocities).

Static data sets

Most of our static data have been collected at the rooftop of the Septentrio building in Leuven, Belgium. Performance data presented in Table 1 for this location reflects a large array of static data with the total length of about a week.

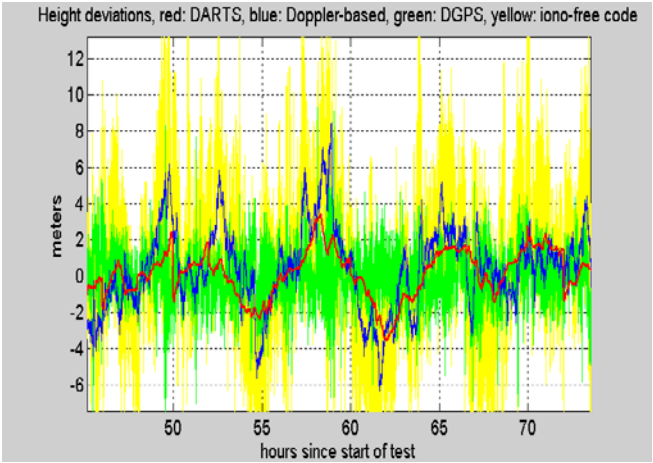

Figure 7. Height deviations of DARTS for a static data set 2003-044 collected at Leuven, Belgium. Red: DARTS; blue: Doppler-aided solution; green: DGPS; yellow: code-only standalone solution.

Height deviations of DARTS for one of the data sets collected at this location are shown in Figure 7. Yellow curve is the un-smoothed iono-free code only solution, affected by both code multipath and system biases. This solution is the noisiest of all presented in this plot. The blue curve corresponds to the real-time solution by the PolaRx receiver, which is using Doppler measurements in order to reduce code multipath noise[4]. It can be seen that the blue curve is quite smooth, but it still follows all the long-term trends of the code-only solution. DARTS solution, the red curve, significantly reduces (roughly by a factor of 2) the magnitude of the deviations caused by system biases. The green curve is a code-based DGPS solution. It can be seen that DARTS solution stays within the error envelope of the DGPS solution. This is a good visual indication that DARTS provides an accuracy, which comes close to the accuracy of DGPS.

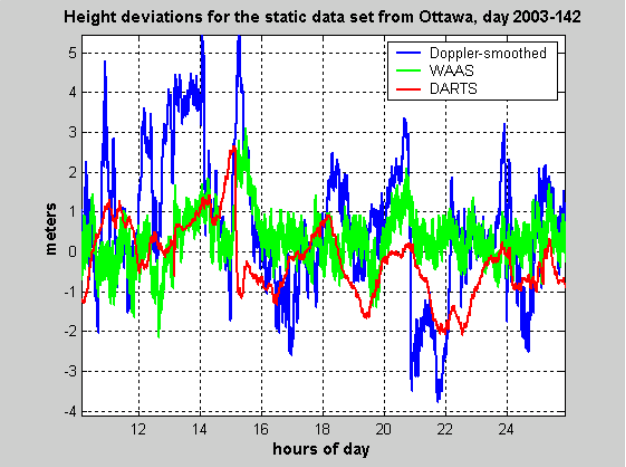

Figure 8. Height deviations of DARTS for a static data set 2003-142 collected at Ottawa, Canada.

Actual relationship between the accuracy of DARTS and the accuracy of DGPS depends mostly upon the magnitude of multipath effects. System biases, which are fully canceled out by DGPS, are only partly compensated by DARTS. Therefore a perfect multipath-free DGPS must have a better performance than DARTS. However, in real-life applications, multipath effects can significantly degrade the performance of DGPS. Therefore, the performance of DARTS, which is almost multipath-free, can be higher in some particular cases than the performance of DGPS.

In this paper we present the comparison of DARTS to code-based DGPS for a few test cases with varying performance of DGPS. Figure 7 shows a raw code-based DGPS in a relatively benign environment, but with no smoothing at all. It can be seen that in this case DARTS and DGPS show a comparable overall performance.

Figure 8 shows positional solutions for another static test data, collected in Ottawa, Canada by Sander Geophysics Ltd, at the company's rooftop. The green curve in this plot is a real-time solution of the PolaRx2 receiver in WAAS mode. Because WAAS corrections are smoothed and the multipath is moderate, the performance of WAAS-assisted solution is higher than the performance of DARTS. An example of an opposite kind will be given later in the section on the container terminal application.

Aircraft test

Aviation applications are known to be relatively benign in terms of multipath and availability of GPS, but they challenge the ability of the algorithm to handle high dynamics and the performance of the tropospheric delay model for a wide range of heights.

An airborne data set collected with PolaRx 2 receiver during a 2-hour-long flight was used for a test. The flight was performed in a mountainous area around Sion in Switzerland on November 18, 2002. The flight was organized by Skyguide (Swiss Air Navigation Services Ltd) and Eurocontrol GNSS Programme (Eurocontrol is a European Organisation for the Safety of Air Navigation). Sion represents quite a challenging environment for satellite navigation solutions being located in the middle of a valley in the heart of the Alps and being surrounded by mountains higher than 4,000 meters. More details on these flights can be found in [5]. The aircraft used was a Dornier DO 128-6, which belongs to the Technical University of Braunschweig, Germany. Equipped with a Septentrio's PolaRx2 GNSS receiver, it flew four experimental approach procedures to the Sion airport. For each approach a variation of heights was between 500 m to 4500 m.

Zimmerwald IGS station was used as a ground station to compute iono-free carrier phase DGPS solution, which was used as reference. Deviations of DARTS and real-time solution of PolaRx2, computed by the Doppler-aided algorithm (refer to [4] for more details on this algorithm) from the reference carrier-phase DGPS solution are presented in Figure 9. RMS positional deviations can be found in the third column of Table 1.

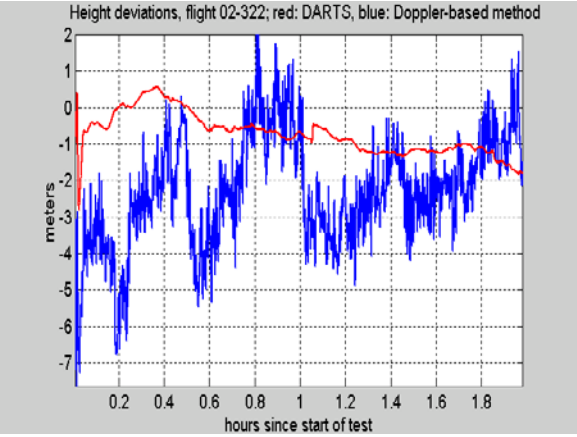

Figure 9. Height deviations for the flight test. Red: DARTS, blue: Doppler-based method.

Figure 9 and Table 1 demonstrate that the performance of DARTS with kinematic data sets is at least not worse than for static data sets. Positional deviations of DARTS most of the time appear as almost constant sub-meter biases. The left edge of the plot shows initialization transient process, which is characteristic for DARTS and lasts about 1 minute. When DARTS initializes, ambiguities are unknown and the position/velocity solution for the first epochs is based on iono-free code only. Then ambiguities are getting more reliable and DARTS-computed position is evolving into a phase-based solution. This process normally takes about 1 minute.

Container terminal application

Figure 10. General view of the Antwerp harbor container terminal with a straddle carrier. An arrow points on top of the straddle carrier, where the GPS antenna is located.

Potential use of GPS to locate containers at the container terminal in the harbor or Antwerp was a subject of the joint project of Septentrio with Hesse Noord Natie, a terminal operator. GPS equipment consisting of the Sensor Systems antenna, the PolaRx2 receiver, and a battery was mounted on the top of the straddle carrier (see Figure 10). The straddle carrier picks up a container after it has been unloaded from the ship and drops it off at the storage location. Later, the straddle carrier will come back to take this container for further handling. The role of GPS positioning in this application is to provide the position of containers at the storage locations (drop-off points) in order to avoid human errors, which may result in the loss of containers.

The kinematic data set was collected during a few hours of normal operation of the straddle carrier. Here we compare post-processed DARTS solution to real-time EGNOS-assisted solution, computed by PolaRx2. Reference iono-free carrier-phase DGPS solution was obtained by post-processing with the BRUS IGS station. The positional deviations for both solutions from the reference are presented in Figure 11and Figure 12.

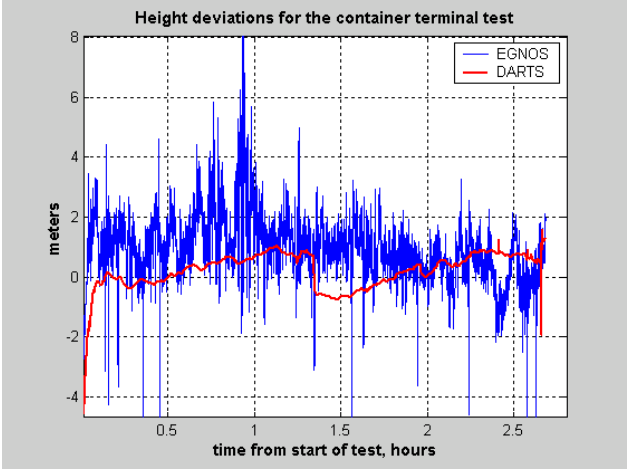

Figure 11. Height deviations for the container terminal test.

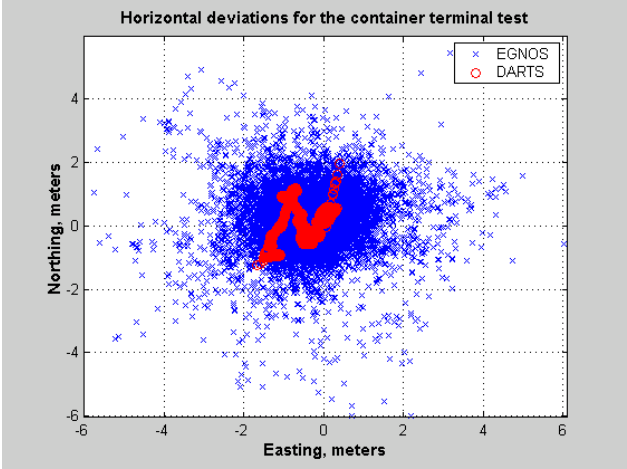

Figure 12. Horizontal deviations for the container terminal test.

The container terminal is an example of an application with good phase tracking, but very high code multipath. Indeed, the top of the straddle carrier is higher than all the containers, that is why satellite availability and continuous phase tracking is quite good. On the other hand, the space of the terminal is so much cluttered with highly reflective metal containers that the STD of C/A code multipath errors reaches the value of 1.1 m, about a double of what is typical for an average urban environment. It is also important that the antenna used for this test is a simple omni-directional antenna with no multipath rejection. Because multipath has a tendency to average out during movement, multipath errors are particularly high at drop-off and pick-up points, where the straddle carrier is static or moves slowly.

Representation of the movement around pick-up and drop-off points is shown in Figure 13, Figure 14. It can be seen that due to severe multipath, which increases when the straddle carrier slows down, the EGNOS-assisted solution performs significantly worse than DARTS. This has nothing to do with the performance of EGNOS itself, which shows sub-meter positional deviations in a more benign environment.

DARTS is not affected by multipath and represents the movement practically in the same way as the reference solution. It can be seen that the DARTS solution is only shifted by an almost constant sub-meter-level bias. For the purposes of container location, sub-meter horizontal accuracy shown by DARTS is more than adequate.

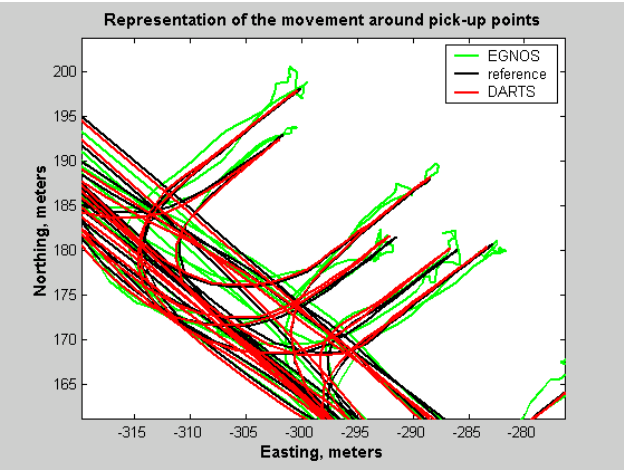

Figure 13. Representation of the movement around pick-up points.

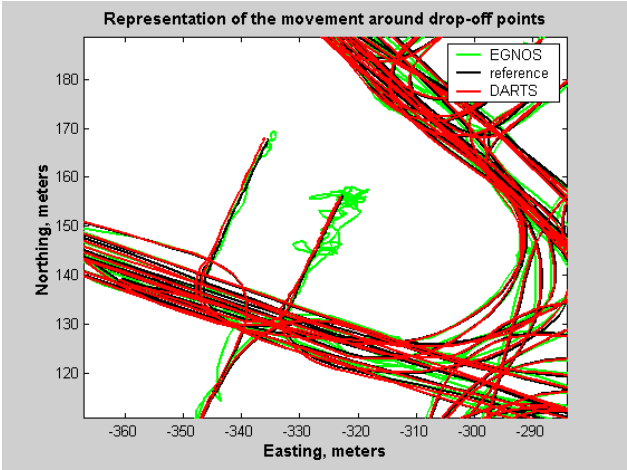

Figure 14. Representation of the movement around drop-off points.

The ability of DARTS to represent small-scale details of the movement to about the same degree of precision as carrier-phase DGPS processing is a natural consequence of the fact that for relatively short periods of time DARTS solution is nothing else but phase processing with somewhat biased ambiguities. Another important reason for an exceptional smoothness of DARTS solution is a good stability of satellite clocks, which short-term noise directly contributes to the error budget of DARTS solution. The smoothness of the DARTS solution and its possible uses are further demonstrated in the next example.

Representation of small-scale movement

Adequate representation of small-amplitude oscillating movement, such as oscillations of bridges or buildings is a serious challenge for standalone positioning due to the adverse effect of short-term code multipath noise. In current practice, applications of this kind mostly use real-time carrier-phase DGPS solutions (RTK). The purpose of this section is to demonstrate that DARTS is fully applicable to applications of this kind because it provides sufficient level of suppression of short-term noise (mostly code multipath errors).

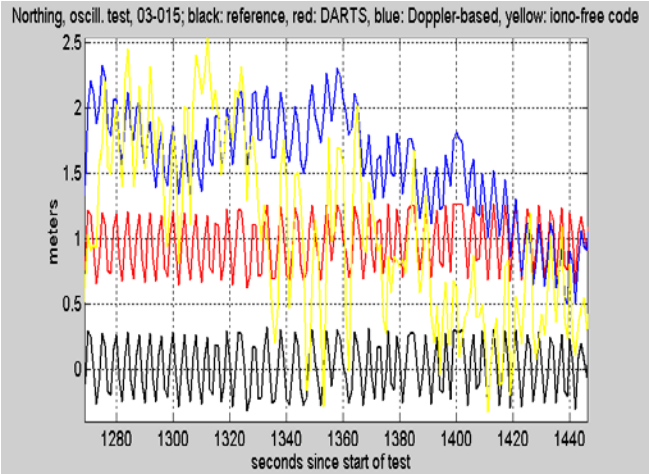

Figure 15. Northing for the small-amplitude movement test. Black: reference (iono-free phase DGPS solution with Brussels IGS station); red: DARTS, blue: Doppler-based solution; yellow: iono-free code standalone solution

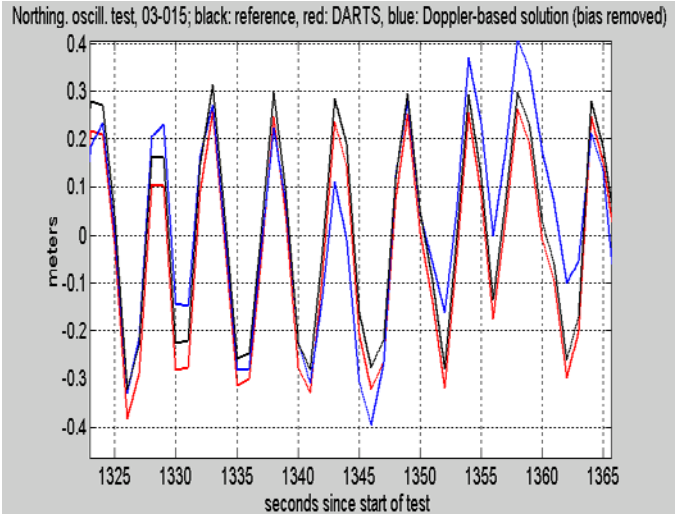

Figure 16. Same as Figure 15, but blue and red curves are shifted in order to coincide with the reference (black)

In our experiment, a GPS antenna was moved by hand in a repeated oscillating pattern with an amplitude of about 50cm in North/South direction. The data were collected by the PolaRx2 GNSS receiver. In Figure 15, the blue curve presents real-time solution by the PolaRx2 receiver, which uses Doppler-based position/velocity algorithm [4]. Other curves are obtained in post-processing.

Four solutions are compared in Figure 15. The lowest, black, curve is the reference; it shows the true pattern of antenna oscillations. Yellow curve is a code-based solution with no smoothing. It can be easily seen that the yellow curve cannot adequately represent the movement, which means that simple code-based solution cannot possibly work in this case. DARTS and Doppler-based method both adequately represent oscillations of the antenna.

DARTS shows a bias of 1 m, which appears to be constant in the time scale of the plot. The bias of this order of magnitude is caused by incomplete compensation of system biases and is normal for DARTS (see Table 1). This plot is a clear illustration of the fact that errors of DARTS appear mostly as a slowly changing bias. In Figure 16 this bias is taken out in order to better demonstrate how well the movement of the antenna is represented. It can be very well seen that DARTS (red curve) represents the oscillations almost perfectly. This proves that DARTS may be considered as an adequate candidate for a number of applications, which are usually considered as belonging to the realm of RTK.

SUMMARY

DARTS is an original standalone navigation algorithm based on combined iono-free code + iono-free phase processing with dynamic ambiguities. It employs a random walk system noise model for ambiguities, which allows for continuous real-time estimation of GPS system biases (orbit and clock errors). DARTS provides a mechanism to partly compensate for the system biases; hence its overall accuracy is comparable to the accuracy of code-differential positioning.

To our knowledge, positional solution of DARTS is the most accurate among all the known real-time standalone algorithms or existing GNSS receivers. DARTS positional solution does not depend upon system dynamics; once stabilized, it is dominated by iono-free phase. Therefore code multipath noise is fully suppressed, and the resulting solution is exceptionally smooth. Millimeter-level velocity noise is a consequence of this smoothness.

DARTS requires initialization period of about 1 minute, which is needed in order to determine ambiguities with sufficient reliability. During this period of time, the positional solution has a transient from code-based to phase-based solution and velocity errors are higher than normal.

It has been demonstrated by a number of examples, both static and kinematic, that DARTS shows stable performance, sub-meter for horizontal coordinates and about one meter for heights. DARTS can be recommended for relatively benign applications where continuous phase tracking is available and accuracies of

this level are sufficient, such as aviation or marine navigation.

FUTURE DEVELOPMENT

For the future implementation in the firmware of the PolaRx2 receiver, DARTS will be augmented in a number of ways. First, the Doppler measurements must be included in the Kalman filter. This will allow for direct computation of velocities from Doppler measurements, which has been shown to significantly increase the robustness of the algorithm in highly dynamic limited visibility environments. More details on Doppler-aiding and possible benefits of its combining with DARTS can be found in [4]. DARTS would also benefit from a more sophisticated error model.

NOTATION

Latin:

A	amplitude of simulated biases
$\hat{A}$	transition matrix of the Kalman filter
$\hat{I}$	identity matrix
$\vec{N}$	ambiguities for all satellites in the solution
q	system noise spectral density
t	time
T	period of simulated biases
$\vec{v}$	vector of velocities $\{v_x, v_y, v_z\}$
w	system noise
$\hat{W}$	system noise matrix
$\vec{x}$	vector of position {x, y, z}
$\vec{X}$	full state vector

Greek:

δ_{prn}	PRN-dependent phase shift for biases
φ	raw phase observable
$\vec{\varphi}$	raw phases for all satellites in the solution
ρ	raw pseudorange observable
$\vec{\rho}$	raw pseudoranges for all satellites in the solution

Indices:

$base$	of a base satellites
$k,k+1$	of the previous and current epochs
x	of kinematic components of the state vector
N	of ambiguity components of the state vector

ACKNOWLEDGEMENTS

I would like to thank my colleague Frank Boon for useful discussions as to the nature of the method and comments on the text.

I am also thankful to:

Jan D'Espallier and Jan Grawen of Septentrio, who have collected a large array of static data and kinematic data, which was instrumental in development and verification of the method;

Steve Ferguson of Sander Geophysics Ltd, for a data set collected at the company's station in Ottawa, Canada;

Frank Wilms of Septentrio who collected the data set at the Antwerp container terminal;

Olivier Perrin of Skyguide and Santiago Soley of the Eurocontrol GNSS Programme for the permission to use their data set collected in the course of ESTB testing;

Technical Department of Hesse-Noord Natie N.V. for co-operation in the Antwerp container terminal project.

REFERENCES

1. Bisnath, S.B. and Langley, R. B. *High-Precision, Kinematic Positioning with a Single GPS Receiver*. NAVIGATION: Journal of the Institute of Navigation, Vol. 49, No. 3, Fall 2002, pp. 161-169.
2. Brown, R.G., and Hwang, P. Y. C. *Introduction to Random Signals and Applied Kalman Filtering*, 2nd edition, Wiley, New York, 1992.
3. Leick, A. *GPS satellite surveying*. 2nd edition, Wiley, New York, 1995.
4. Simsky, A. and Boon, F. *Carrier phase and Doppler-based Algorithms for Real-Time Standalone Positioning*. Proceedings of the GNSS 2003, The European Navigation Conference 22-25 April/Graz, Austria.
5. Perrin, O., Scaramuzza, M., Buchanan, T., Soley, S., Gilliéron, P.-Y., Waegli, A., *Challenging EGNOS in Swiss Alps*. Proceedings of the GNSS 2003, The European Navigation Conference 22-25 April/Graz, Austria.